DOI: 10.1002/adma.200700414

Octupolar Films with Significant Second-Harmonic Generation**

By *Mi-Yun Jeong*, *Hwan Myung Kim*, *Seung-Joon Jeon*, *Sophie Brasselet*,* and *Bong Rae Cho**

Considerable efforts are being made to develop octupolar nonlinear optical materials for possible application in optical and electro-optical devices.[1–3] An advantage of such molecules in comparison to the more conventional dipolar molecules is the existence of a broader range of tensorial coefficients, providing optimum nonlinear efficiency with a polarization-independent second-harmonic response with respect to the incident light. Great progress has been made by optimization at the molecular level, as exemplified by the established structure–property relationship of two-dimensional octupoles and the development of highly efficient molecules.[3–5] Recently, we reported that 1,3,5-tricyano-2,4,6-tris(*p*-diethylaminostyryl)benzene (TTB) produces non-centrosymmetric crystals that show very large second-harmonic generation (SHG).[1] To integrate such materials in optical devices, it is essential to prepare thin films showing large SHG and high thermal stability. As electric poling is not possible because of the lack of a ground-state dipole moment, it is not readily obvious how to align octupolar molecules non-centrosymmetrically in a thin film. Although optical poling in polymers has been proposed, it requires photoisomerizable molecular functions and resonant excitation of the molecules by intense laser pulses, which may be a limitation for industrial application. An ideal solution to this problem would be to prepare self-oriented films without applying external fields. For this purpose, we have studied thin films of TTB in a polymethylmetacrylate (PMMA) matrix prepared by using free-casting and spin-coating methods, and measured their SHG at 1064 and 1560 nm. We have achieved, for the first time, non-centrosymmetric deposition of octupoles in thin films with a non-negligible efficiency. This work describes the structural and optical properties of such films. The films (10 and 20 wt % TTB/PMMA) were prepared by depositing a solution of TTB and PMMA in chlorobenzene on cleaned glass plates (BK7) of 1 mm thickness (ca. $\lambda/10$ roughness) by using free-casting and spin-coating methods.

The absorbance spectrum of the spin-coated film is nearly identical to that of the solution, whereas that of the free-cast film is broad (Supporting Information, Fig. S1). This indicates that the former is uniform and possibly amorphous, whereas the latter most probably contains microdomains that scatter the light and thus broaden the spectrum.

Polarizing microscope images of the free-cast films are shown in Figure 1 and the Supporting Information, Figure S2. They reveal bright and dark domains. The domains look like weaved fibrous tissues showing various patterns, such as stacked leaves, triangles, and polyhedrons, of 0.1–2 mm in size. The thickness of the film is uniformly around 1 μm. When the film is rotated by approximately 45°–50° in its plane, the bright domains turn dark, and vice versa, indicating that such domains are aligned in different polarization directions. In contrast, no such domains were observed in the spin-coated films, which confirms their amorphous nature.

The existence of crystalline domains in the free-cast film is clearly demonstrated by X-ray diffraction (XRD) spectra (Fig. 1c–e). The spectra for the powder sample and free-cast film coincide at $2\theta = 5.86$ and 11.72, which corresponds to repeating units of 15 and 7.5 Å, respectively. The former is nearly identical to the length of a branch of the TTB molecule from its center as determined by X-ray crystallography, whereas the latter is somewhat larger than the centroid separation between TTB molecules (ca. 5 Å) in the unit cell.[1] Because the unit cell consists of three molecules packed along *c*-axis with a slight offset, the most likely structure of the crystal domain appears to be a cylinder, in which the TTB planes are stacked with a separation of 7.5 Å (Fig. 2).

The SHG and two-photon excited fluorescence (TPEF) spectra of the free-cast film is shown in the Supporting Information, Figure S3. When pumped at 1064 nm, the film emits intense SHG at 532 nm along with a weak TPEF at 620 nm. Similar results were observed with 1560 nm laser photons as the pump beam. Interestingly, the TPEF from the crystal is almost completely quenched in the PMMA matrix. Hence, all of the photons collected at 532 and 780 nm are entirely due to SHG. In contrast, the spin-coated film showed no peak in the

[*] Dr. S. Brasselet[+]
Laboratoire de Photonique Quantique et Moléculaire
Ecole Normale Supérieure de Cachan
61 avenue du president Wilson, 94235 Cachan (France)
E-mail: sophie.brasselet@fresnel.fr
Prof. B. R. Cho, H. M. Kim, Prof. S.-J. Jeon
Molecular Opto-Electronics Laboratory
Department of Chemistry
Korea University, 1-Anamdong, Seoul 136-701 (Korea)
E-mail: chobr@korea.ac.kr
Dr. M.-Y. Jeong[++]
Department of Physics
Korea University
1-Anamdong, Seoul 136-701 (Korea)
[+] Present address: Institut Fresnel, MOSAIC group, Domaine Univ. St Jerome, 13397 Marseille Cedex 20, France.
[++] Present address: Department of Physics, Ewha Womans University, Seoul 120-750, Korea.
[**] We acknowledge financial support from KOSEF (2006-03792).

ADVANCED MATERIALS

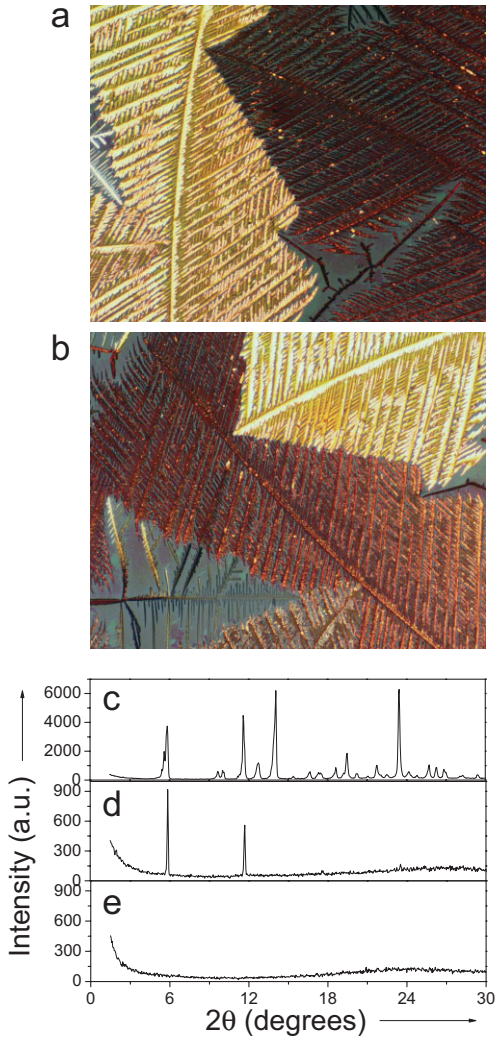

Figure 1. Polarizing microscopy images of a) 10 wt% TTB/PMMA film with a magnification factor of 100, b) the same film rotated at 45°, and XRD spectra of c) TTB powder, d) free cast, and e) spin-coated films (10 wt% TTB/PMMA).

XRD spectrum and no SHG, as expected. This indicates that the film is amorphous and that crystal domains must be present to exhibit SHG.

Nonlinear optical efficiencies of a crystal are defined by the nonlinear susceptibility tensor d, which is deduced from the oriented gas model.[6] Assuming an octupolar symmetry for the TTB crystal and adopting the model developed by Zyss et al.,[7] the only nonvanishing coefficients in the (1,2,3) unit-cell framework are $d_{111} = Nf_1^{2\omega}(f_1^{\omega})^2\beta_{111}$, $d_{122} = -Nf_1^{2\omega}(f_2^{\omega})^2\beta_{111}$, and $d_{212} = d_{221} = Nf_2^{2\omega}f_1^{\omega}f_2^{\omega}\beta_{111}$, where N is the number density of the TTB molecule. The local-field correction factors f_i are determined according to the Lorentz–Lorentz model with $f_i^{\omega} = ((n_i^{\omega})^2 + 2)/3$, where n_i^{ω} is the refractive index at frequency ω. Because of the trigonal symmetry of the in-plane structure of the TTB crystal, $n_1^{\omega} = n_2^{\omega}$, and $d_{111} = -d_{122} = -d_{212} = -d_{221} = \|(d)\|/2$ where $\|(d)\| = \sqrt{(\sum_{i,j,k} d_{ijk}^2)}2$ is the norm of the d tensor.[1]

SHG signals present the advantage of being sensitive to crystal structure, orientation, as well as incoming field polarization. To determine the domain structure by using SHG polarized responses, an incoming beam at 1064 nm (or 1560 nm) of linear polarization was used to illuminate a crystal domain in the free-cast film along the Z direction, while rotating the polarization angle $\Phi = (X, E^{\omega})$ from 0° to 360° (Fig. 2 and Supporting Information, Fig. S4a). The focused beam with ca. 400 μm in diameter and 0.96 μm in thickness illuminated one crystalline domain with ca. 1 mm in diameter. As shown in Figure 3a and b, the polar diagrams show two-lobe patterns at both 1064 and 1560 nm wavelengths. This indicates that the TTB planes are located perpendicular to the (X, Y) plane, $\theta(Z, z) = 90°$ (with notations defined in Fig. 2b). We have

$$d_{IJK}(\phi, \psi) = \sum_{i,j,k=1,2} d_{ijk}\left(\vec{U}_i \cdot \vec{U}_I\right)\left(\vec{U}_j \cdot \vec{U}_J\right)\left(\vec{U}_k \cdot \vec{U}_K\right)(\phi, \psi) \quad (1)$$

with $I, J, K = X, Y$

$$\vec{U}_1 = -\sin\psi \sin\phi\ \vec{U}_X + \sin\psi \cos\phi\ \vec{U}_Y - \cos\psi\ \vec{U}_Z \quad (2)$$

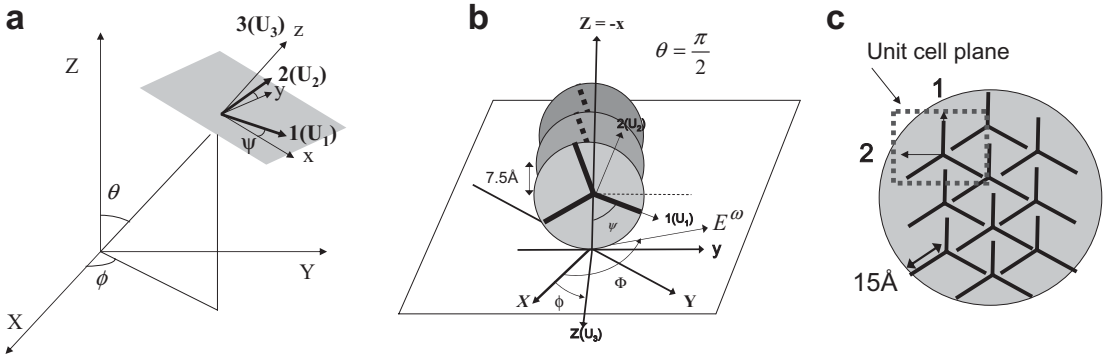

Figure 2. a) Definition of the Euler angles (θ, ϕ, ψ) in the laboratory coordinate (X, Y, Z) and the molecular coordinate (1, 2, 3). The (θ, ϕ) angles define the orientation of the x,y molecular plane in the laboratory coordinate. b) Orientation of the hexagonal columnar structure of TTB crystal domain in the film. c) Arrangement of TTB molecules, in the hexagonal plane, lie in the x,y plane, with an orientation angle ψ between the x- and 1-axes as shown in b).

$$\vec{U}_2 = -\cos\psi \sin\phi \vec{U}_X + cos\psi \cos\phi \vec{U}_Y + sin\psi \vec{U}_Z \quad 3$$

and

$$\vec{E}^{\omega}(\Phi) = \cos\Phi \vec{U}_X + \sin\Phi \vec{U}_Y \quad 4$$

Note that in the case of an incoming field along X ($\Phi = 0°$), $I_{X,Y}{}^{2\omega}(\phi,\psi,0)$ takes a simple form that leads to a ratio independent of ψ

$$I_X^{2\omega}(\phi,\psi,\Phi=0) = |d_{111}\cdot I_X^{\omega|2}\cdot\left(\sin^3\psi - 3\cos^2\psi\sin\psi\right)^2\cdot\sin^6\phi \quad 5$$

$$I_Y^{2\omega}(\phi,\psi,\Phi=0) = |d_{111}\cdot I_X^{\omega|2}\cdot\left(\sin^3\psi - 3\cos^2\psi\sin\psi\right)^2\cdot\sin^4\phi\cos^2\phi \quad 6$$

$$I_X^{2\omega}(\phi,\psi,0)/I_Y^{2\omega}(\phi,\psi,0) = \tan^2\phi \quad 7$$

The $I_X{}^{2\omega}/I_Y{}^{2\omega}$ ratio, at an of angle $\Phi = 0$, determined from Figure 3a, is 7.49/1.07, from which $\phi = 69.2°$ is calculated. This indicates that the molecular plane x–y is tilted from the X–Z plane by 69.2°. For the 780 nm measurement, $I_Y{}^{2\omega} = 0$ and $I_X{}^{2\omega}$ were also fitted from Figure 3b using Equation 7. This indicated that $\phi = 90°$, which means that the molecular plane x–y is parallel to the X–Z plane. The discrepancy between the

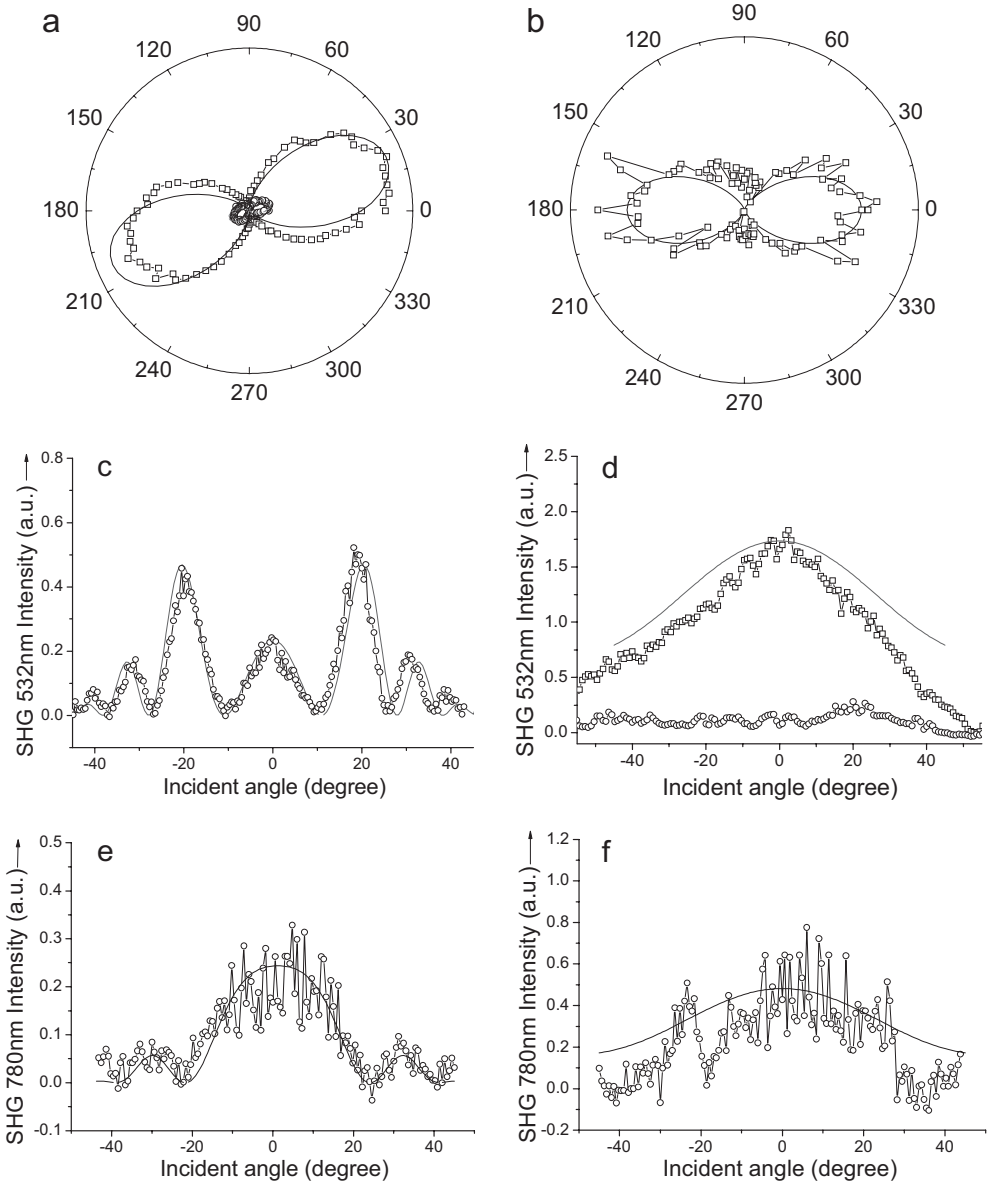

Figure 3. Polar diagrams representing the SHG of a domain of 10 wt % TTB/PMMA film measured at a) 532 nm and b) 780 nm, as a function of the incident polarization angle. Maker Fringe patterns of Y-cut Quartz measured at c) 532 nm and e) 780 nm, and of the film measured at d) 532 nm and f) 780 nm. In all cases, the experimental data (open circles) fit well to the theory (solid line). From the polar plot and the Maker fringe results, the Euler angles (θ, ϕ, ψ) of the domain are determined as (90°, 21°, 3°) at 532 nm and (90°, 0°, 3o) at 780 nm.

ADVANCED MATERIALS

ϕ values measured at the two wavelengths is due to the different alignments of the films in the two experiments. Consistently, when the sample domain was rotated by 90° in the X–Y plane, the two-lobe pattern rotated by 90° with concomitant exchange of $I_X^{2\omega}(=0)$ and $I_Y^{2\omega}$. Similar results were observed for 20 wt % TTB/PMMA film (Supporting Information, Fig. S5a).

The general fit of Figure 3a and b for a varying Φ angle shows excellent agreement between the experimental data and theoretical model, demonstrating the validity of this analysis and especially the geometry of the structure of the molecular arrangement. The polarization responses represented as polar plots in Figure 3a and b are representative of octupoles lying perpendicular to the plane in which the fundamental incident polarization is rotated. Indeed in such a configuration, molecular-field coupling takes place perpendicularly to the octupole planes, which explains the "dipole-like" two-lobe pattern of the polarization response. Such features have also been observed in bulk TTB crystals.[1]

In order to determine the tilt angle ψ, we performed Maker fringe experiments[8,9] locally in the domains of the thin films. Figure 3c and d show the Maker fringes of Y-cut Quartz crystal and a domain of the film with ca. 1 mm in diameter measured with a focused beam size of about 400 μm at 532 and 780 nm.

Assuming octupolar symmetry for the crystal domain, d_{eff}^2 measured in a Maker fringe configuration (Supporting Information, Fig. S4b for coordinates) can be expressed for the P-polarized input-pump beam ω and the P-polarized output beam 2ω, as

$$d_{eff}^2 = d_{111}^2[(S_1^2 - C_1^2)C_2 - 2(C_1 \cdot S_1)S_2]^2 \quad 8$$

where $S_1 = \sin(\theta_\omega + \psi)$, $c_1 = \sqrt{(1 - S_1^2)}$, $S_2 = \sin(\theta_{2\omega} + \psi)$, $c_2 = \sqrt{(1 - S_2^2)}$, $\theta_\omega = \sin^{-1}((1/n_\omega)\sin\theta)$, and $\theta_{2\omega} = \sin^{-1}((1/n_{2\omega})\sin\theta)$, n_ω is the refractive index of the film at ω, $n_{2\omega}$ is the refractive index of the film at 2ω, and θ is the incident angle of the pump beam. Using this expression, ψ could be determined from the angle where the maximum intensity value is

$$P_{2\omega,\max}^{p\to p} \quad 9$$

obtained with $\psi = 3°$ both at 532 and 780 nm (Fig. 3d and f). The features shown in Figure 3 are in fact envelop fringes, because the thickness of the film is much smaller than the coherence lengths for SHG (which are 4.3 μm at 1064 nm and 32 μm at 1560 nm, estimated from indexed data in bulk TTB crystals).

In addition to structural information, the Maker fringe experiment allows us to determine a quantitative value for the nonlinear coefficients in the thin film. A generalized version of Herman and Hayden's theory[8,9] was used to calculate the second-order nonlinear optical coefficient d_{111}. The thickness and refractive indices of quartz and the film used for the calculation were as follows: the quartz thickness was 990 μm and the film thickness was 0.96 μm; the refractive indices at 532, 780, 1064, 1560 nm were 1.54690, 1.53878, 1.53410, and 1.52735 for Quartz[10] and 1.6720, 1.6110, 1.5167, and 1.3025 for the film (see the Supporting Information, Fig. S6).[11,12] In all cases, the experimental data were in reasonable agreement with the theoretically fitted curves (Fig. 3d and f). Moreover, the calculated second-order NLO coefficient of the free-cast film was found to be $d_{111} = 11.8$ pm V^{-1} (28.2×10^{-9} esu; 1 esu = 3.33564×10^{-10} C) at 1064 nm and $d_{111} = 14.6$ pm V^{-1} (34.9×10^{-9} esu) at 1560 nm. The comparison of these two values cannot be directly made because the first value is expected to originate from resonance conditions, where both enhancement and reabsorption of the second harmonic are expected. Indeed, the absorption coefficient of the film at 780 nm is 0.02, an order of magnitude lower than 0.25 at 532 nm (Supporting Information, Fig. S1). Consequently, the nonlinear coefficients corrected for the absorption are 21.1 pm V^{-1} at 1064 nm and 15.3 pm V^{-1} at 1560 nm, respectively, which confirms the resonance of the nonlinear process at 1064 nm. The second value is therefore more reliable as close to a nonresonant nonlinearity, because in this case 2ω lies away from the maximum of absorption of the film.

We also measured the SHG of 20 wt % TTB/PMMA film (thickness 0.377 μm) at 1560 nm by using the same method (Supporting Information, Fig. S5b). The d_{111} value, calculated by using the same refractive indices as above, was 22.4 pm V^{-1} (53.3×10^{-9} esu). The larger d_{111} value in this film is in part attributed to the increased number density of the TTB molecules. Alternatively, higher TTB concentration may have provided a more favorable crystallization condition in the PMMA matrix to produce a domain with higher number density than expected from the concentration of the stock solution. For comparison, the $\|d\|$ value for TTB bulk crystal, measured with femtosecond pulses at 1028 nm, is 1580×10^{-9} esu, which is larger by about two order of magnitude than that in the films. In addition to the uniformly high efficiency of the nonlinearity within the film domains, the characteristics of the molecular off-plane orientation ($\theta = 90°$) was seen to be the same for all observed domains in the films, confirming the cylindrical symmetry within each domain and the uniformity of the molecular behavior.

The origin of this difference is not completely elucidated, but could be due to the difference in the structures: a uniform crystalline matrix in the bulk crystal and a conjunction of domains of possibly different in-plane orientations in the thin films. Nevertheless, the d_{111} value measured for 20 wt % TTB/PMMA film is close to the 30 pm V^{-1} required for industrial applications. Moreover, the films were stable for 1 year at room temperature and 3 days at 100 °C.

In summary, we have prepared thin films of TTB/PMMA by using free-casting and spin-coating methods. The physical properties of the films were examined by using absorption spectra, polarization microscopy, XRD, and SHG. The free-cast films have crystal domains that have hexagonal columnar structure and show significant SHG and high thermal stability. These films will ultimately be useful in nonlinear-optics applications.

Experimental

Preparation of the Film: A mixture of TTB (0.10 g, 1.5×10^{-4} mol) and PMMA (molecular weight, $M_W = 100\,000$, 0.90 g) was dissolved in chlorobenzene (17 mL). The solution was filtered with a 0.2 μm Teflon filter and a few drops of the solution were placed on BK7 plates (ca. $\lambda/10$ roughness). The deposited plates were covered with glass caps and kept for 1 week at room temperature to evaporate the solvent. A 20 wt % TTB/PMMA film was prepared by using the same procedure except that larger amounts of TTB (0.8 g, 8×10^{-6} mol) were used. Alternatively, a few drops of the solution were spin-coated on the same plates at 1000 rpm, kept for 1 day at ambient temperature, and then placed in a vacuum oven for 3 days at 100 °C to completely evaporate the solvent.

Polarizing Microscope: The film was placed between a polarizer and analyzer with the polarization direction placed perpendicularly. Images were obtained by rotating the film by approximately 45°–50°.

Optical Measurements: For SHG measurements, the 1064 nm beam was obtained from an Nd:YAG laser (10 Hz, Q-switched, pulse width, 7 ns) and the 1560 nm beam was obtained from the stimulated anti-Stokes Raman scattering of a 1064 nm beam from a Raman cell (D_2, 40 kg cm^2). The laser beam was passed through a polarizer, $\lambda/2$ plate, and high-pass filter before irradiating the film, by using the experimental setup shown in Figure S4 (Supporting Information). The beam polarization angle was varied by rotating the $\lambda/2$ plate in 3.2° increments by using the step motor. Each SHG data point is an average of at least 50 and 120 measurements for 532 and 780 nm, respectively. To determine d_{111}, Y-cut Quartz was used as a reference.

Measurement of the Refractive Index: The refractive indices of the films were determined by using the ellipsometer (USA, J. A. Woollam VUV- VASE UV-302) following the procedure from the literature [11,12]. The wavelength dependency of the refractive indices is shown in Figure S6.

Received: February 15, 2007
Revised: March 24, 2007
Published online: July 17, 2007

[1] V. Le Floc'h, S. Brasselet, J. Zyss, B. R. Cho, S. H. Lee, S.-J. Jeon, M. Cho, K. S. Min, M. P. Suh, *Adv. Mater.* **2005**, *17*, 196.
[2] M. J. Lee, M. J. Piao, M.-Y. Jeong, S. H. Lee, S.-J. Jeon, T. K. Lim, B. R. Cho, *J. Mater. Chem.* **2003**, *13*, 1030.
[3] H. C. Jeong, M. J. Piao, M.-Y. Jeong, K. M. Kang, G. Park, S.-J. Jeon, B. R. Cho, *Adv. Functional Mater.* **2004**, *14*, 64.
[4] C. Dhenaut, I. Ledoux, I. D. W. Samual, J. Zyss, M. Bourgault, H. L. Bozec, *Nature* **1995**, *374*, 339.
[5] V. R. Thalladi, S. Brasslet, H.-C. Weiss, D. Blaser, A. K. Katz, H. L. Carrell, R. Boese, J. Zyss, A. Nangia, G. R. Desiraju, *J. Am. Chem. Soc.* **1998**, *120*, 2563.
[6] J. Zyss, S. Brasselet, V. R. Thalladi, G. R. Desiraju, *J. Chem. Phys.* **1998**, *109*, 658.
[7] J. Zyss, S. Brasselet, V. R. Thalladi, G. R. Desiraju, *J. Chem. Phys.* **1998**, *109*, 658.
[8] W. N. Herman, L. M. Hayden, *J. Opt. Soc. Am. B* **1995**, *12*, 416.
[9] T. K. Lim, M.-Y. Jeong, C. Song, D. C. Kim, *Applied Opts.* **1998**, *37*, 2723.
[10] http://www.cvilaser.com/Common/PDFs/Index_of_Refraction.pdf (accessed July 2007).
[11] H. G. Tompkins and W. A. McGahan, *Spectroscopic Ellipsometry and Reflectrometry*, Wiley Press, New York, **1999**.
[12] A. Alvarez-Herrero, H. Guerrero, E. Bernabeu, D. Levy, *Appl. Opt.* **2002**, *41*, 6692.